Received: 5 November 2019 | Revised: 28 January 2020 | Accepted: 10 February 2020

DOI: 10.1111/jce.14394

WILEY

ORIGINAL ARTICLE

Impact of atrial programmed electrical stimulation techniques on unipolar electrogram morphology

Paul Knops BSc[1] | Corina Schram-Serban MSc, DVM[1] | Lisette van der Does MD[1] | Marshall Croes BSc[1] | Richard Houben MSc[2] | Natasja de Groot MD, PhD[1]

[1]Department of Cardiology, Erasmus Medical Center, Rotterdam, The Netherlands

[2]2BMedical, Maastricht, The Netherlands

Correspondence
Natasja de Groot, MD, PhD, Department of Cardiology, Erasmus Medical Center, PO Box 2040, 3000 CA Rotterdam, The Netherlands.
Email: n.m.s.degroot@erasmusmc.nl

Funding information
Biosense Webster,
Grant/Award Number: IIS-331-1

Disclosures: None.

Abstract

Introduction: Intra-atrial conduction abnormalities are associated with the development of atrial fibrillation (AF) and cause morphological changes of the unipolar atrial electrogram (U-AEGM). This study examined the impact of different atrial programmed electrical stimulation (APES) protocols on U-AEGM morphology to identify the most optimal APES protocol provoking conduction abnormalities.

Methods: APES techniques (14 protocols) were applied in 30 patients referred for an electrophysiology study, consisting of fixed rate, extra, and decremental stimuli at different frequencies. U-AEGM morphologies including width, amplitude, and fractionation for patients without (control group) and with a history of AF (AF group) were examined during APES. In addition, sinus rhythm (SR) U-AEGMs preceding different APES protocols were compared to evaluate the morphology stability over time.

Results: U-AEGM morphologies during SR before the APES protocols were comparable (all $P > .396$). Atrial refractoriness was longer in the AF group compared to the control group (298 ± 48 vs 255 ± 33 ms; $P \leq .020$), but did not differ between AF patients with and without amiodarone therapy (278 ± 48 vs 311 ± 40 ms; $P \geq .126$). Compared to the initial SR morphology, U-AEGM width, amplitude, and fractionation changed significantly during the 14 different APES protocols, particularly in the AF group. In both groups, U-AEGM changes in morphology were most pronounced during fixed-rate stimulation with extra stimuli (8S1-S2 = 400-250 ms).

Conclusion: APES results in significant changes in U-AEGM morphology, including width, amplitude, and fractionation. The impact of APES differed between APES sequence and between patients with and without AF. These findings suggest that APES could be useful to identify AF-related conduction abnormalities in the individual patient.

KEYWORDS

atrial fibrillation, atrial programmed electrical stimulation, conduction abnormalities

1 | INTRODUCTION

Intra-atrial conduction abnormalities are the main features of the electropathological substrate underlying persistence of atrial fibrillation (AF).[1] High-density epicardial mapping studies have demonstrated that intra-atrial conduction abnormalities are expressed in the morphology of the unipolar atrial electrogram (U-AEGM).[2-6] Conduction abnormalities during sinus rhythm (SR)

mainly occur at specific locations or maybe predominantly masked due to nonuniform anisotropic tissue properties.[7,8] Dedicated electrical stimulation techniques, which have the advantage of providing a stable and repetitive heart rhythm, may unmask areas of conduction abnormalities.[9-14] However, which programmed electrical stimulation technique is most optimal for provoking intra-atrial conduction abnormalities is still unknown.[15]

We hypothesize that different atrial programmed electrical stimulation techniques (APES) reveal intra-atrial conduction abnormalities to a variable degree. The aim of this study is, therefore, (a) to investigate the impact of various stimulation techniques on the U-AEGM morphology of patients without (control group) and with a history of AF (AF group), and (b) to identify the most optimal APES sequence to unmask intra-atrial conduction abnormalities.

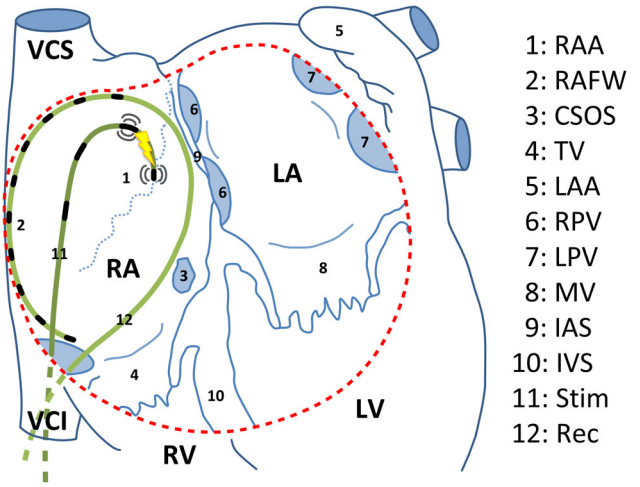

FIGURE 1 Anatomy and catheter positions. Schematic picture of the heart with positions of the stimulation and recording catheters inserted in the right atrium at the start of the electrophysiological procedure. The anterior wall has been partially removed to visualize the inside of the atria. Stimulation was applied from the distal electrode pair of the stimulation catheter (11), positioned in the RAA. Recordings were taken from the recording catheter (12) placed in the RAFW region. CSOS, coronary sinus ostium; IAS, interatrial septum; IVS, interventricular septum; LA, left atrium; LAA, left atrial appendage; LPV, left pulmonary veins; LV, left ventricle; MV, mitral valve; RA, right atrium; RAA, right atrial appendage; RAFW, right atrial free wall; Rec, recording catheter; RPV, right pulmonary veins; RV, right ventricular; Stim, stimulation catheter; TV, tricuspid valve; VCI, inferior caval vein; VCS, superior caval vein

2 | METHODS

2.1 | Study population

The study population consisted of patients scheduled for an electrophysiology study and if applicable ablative therapy. As programmed electrical stimulation is a part of a normal electrophysiological study before ablative therapy and standard techniques and equipment were used, the Erasmus MC medical ethics committee decided written consent from the participants was not required (MEC-2014-511).

2.2 | Materials

After femoral vein access, a standard diagnostic quadri- or hexapolar catheter (M0045291S0, 6F Explorer 360, 2-mm band electrodes, 5-mm electrode spacing; Boston Scientific Corporation [BSCI], San Jose, CA, or 401271, 6F Response, 2-mm band electrodes, 5-mm electrode spacing, St. Jude Medical [SJM], Minnetonka, MN) was positioned in the right atrial auricle (RAA). A standard diagnostic decapolar catheter (M0047000D0, 6F Polaris X, 1-mm band electrodes with 2.5 mm interelectrode distance; BSCI) was placed clockwise across the right atrial free wall (RAFW). Catheter positions were confirmed with fluoroscopic images using left and right anterior oblique views. Figure 1 shows a schematic representation of the catheter positions during the electrophysiology study.

2.3 | Signal recording and APES protocols

From each electrode of the decapolar RAFW catheter, unipolar signals were recorded at 2-kHz sampling rate by the EP-WorkMate Recording System V4.3.2 (SJM, St. Paul, MN), while APES was performed from the distal electrode pair of the RAA catheter with an integrated EP-4 clinical stimulator (EP MedSystems, West Berlin, NJ). Before recording, stimulation configurations were tested for atrial capture and thresholds (milliamperes, mA). APES output was programmed at least 2 mA above a threshold value to ensure atrial capture.

Signals were filtered with 0.05 to 500 Hz filter and amplified to 1 mV/cm. The patient's leg, or the proximal hexapolar catheter electrode in the inferior caval vein if available, was used as an indifferent electrode. Einthoven's ECG lead II served as a reference for the timing of the ventricular activity.

Signals were recorded during SR and during specific APES protocols at different sequences and frequencies, including fixed-rate stimulation without and with extra stimuli and decremental stimulation, as summarized in the left side of Table 1. Between the subsequent protocols, the APES was interrupted to allow the recovery of the intrinsic SR. Protocols with longer APES than SR cycle length (CL) were off course excluded. When atrial refractoriness (AR; defined as the failure to excite atrial tissue) was reached or fusion of the APES U-AEGM with far-field R waves (FFRW) occurred, the specific protocol was repeated once for confirmation.

Each sequence of the APES protocol was exported in binary format (2 byte integer, 1 μV/least significant bit), converted and imported in custom-made MATLAB software (MathWorks, Natick, MA) for further analysis.

TABLE 1 Effectiveness of the various atrial programmed electrical stimulation protocols

	Stimulation protocol		Usable recordings	Not usable recordings due to (n)				
No.	Maneuver	Sequence, ms	(n (%))	NA	BCL ≤ 600 ms	AR[a]	FFRW[a]	Induced AF
Baseline SR								
1		…	30 (100)					
Fixed-rate stimulation (S1)								
2		BCL −50	[b]	23 (77)	5	2		
3		500	29 (97)	1				
4		400	29 (97)	1				
5		300	27 (90)	1		2		
Fixed-rate stimulation with single extra (8S1-S2)								
6		600-350	27 (90)	1	1		1	
7		600-300	22 (73)	2	2	4		
8		600-250	11 (37)	4	2	11[c]	1	1
9		500-350	29 (97)	1				
10		500-300	24 (80)	1		4	1	
11		500-250	15 (50)	1		12[c]	1	1
12		400-350	24 (80)	4		1[d]	1	
13		400-300	24 (80)	2		3[d]	1	
14		400-250	15 (50)	2		8	4	1
Decremental stimulation (−50 ms decrement)								
15		600-550-500-…-200	27 (90)	2	…	…	…	1
15 protocols × 30 pts = 450 attempts		356 (79)	28	7	45[a]		10	4

Note: Left column: details of the applied APES protocols, middle column: total number of recordings that could be used for U-AEGM analysis for every APES protocol separately. Right columns: the number of recordings that could not be used due to BCL ≤ 600 ms, AR, FFRW, or induced AF.
Abbreviations: AF, atrial fibrillation; AR, atrial refractoriness; BCL, basic cycle length; FFRW, far-field R wave; NA, not available; SR, sinus rhythm; U-AEGM, unipolar atrial electrogram.
[a]In case of combined occurrence of AR and FFRW, AR was counted.
[b]Minimal 550 ms.
[c]In case of combined occurrence of AR and FFRW, AR was counted (including 2× FFRW).
[d]In case of combined occurrence of AR and FFRW, AR was counted (including 1× FFRW).

2.4 | Description of the U-AEGM morphology

Widths, amplitudes, and fractionation of SR and APES U-AEGM were examined as displayed in the upper panel of Figure 2. The width of the U-AEGM (milliseconds, ms) was measured between the first and the last deviation from the baseline and the amplitude (milliVolts, mV) between the most positive and negative peak. Fractionation was defined as the presence of two or more negative deflections, as previously described.[16,17]

2.5 | Comparison of U-AEGM morphologies between SR and APES

For every patient, U-AEGM morphologies obtained during SR before initiation of each different APES protocol were compared for each individual electrode to assess the stability of the U-AEGM morphology over time.

The impact of different APES protocols on U-AEGM morphologies was examined by calculating differences between SR and APES U-AEGM widths, amplitudes, and fractionation. The U-AEGM morphology obtained during SR was compared with the (a) APES U-AEGM morphology (S1) during fixed-rate stimulation, (b) extra stimuli (S2) U-AEGM morphology during fixed-rate stimulation with extra stimuli, and (c) U-AEGM morphology of the last captured APES beat during decremental stimulation.

Changes in U-AEGM morphology during the specific APES protocols were evaluated for the entire patient group as well as for the control group and the AF group separately, when appropriate. Subsequently, the APES protocols resulting in the most significant changes in the U-AEGM morphology were identified.

2.6 | Statistical analysis

Statistics were performed with Excel 2010 (Microsoft Corporation, Redmond, WA) and SPSS Statistics 24 (IBM Corporation, Armonk, NY). Normality was tested using the Shapiro-Wilk test. Normally distributed variables were presented by mean ± SD, or by median (minimum-maximum) when skewed and compared by Student *t* or Mann-Whitney U test. Numerical data were assessed

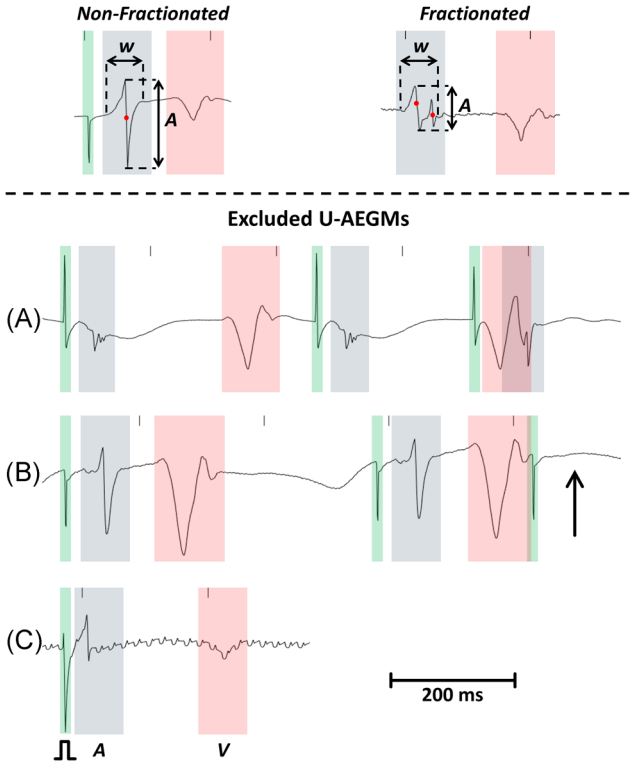

FIGURE 2 Analysis of U-AEGM Morphology. Upper panel: examples of width (w) and amplitude (A) measurements in nonfractionated and fractionated U-AEGMs. The width of the U-AEGM is defined as the duration from the first deviation from the baseline until it returns to the baseline, whereas the amplitude is the voltage difference between positive and negative peaks. Red dots mark the negative slopes of the U-AEGMs. When two or more negative slopes were present, the U-AEGM was labeled as fractionated. See the text for further explanation. Lower panel: (A) fusion of the U-AEGM after S2 extra stimulus with the FFRW in the third electrogram, (B) the arrow indicates AR occurring after S2 extra stimulus, and (C) U-AEGM with the low signal-to-noise ratio. Green, blue, and red rectangles in the U-AEGM tracings represent, respectively, the windows of stimulation artifact (∏), the U-AEGM (A), and the FFRW signal (V). AR, atrial refractoriness; FFRW, far-field R waves; U-AEGM, unipolar atrial electrogram

TABLE 2 Demographic and clinical data

Characteristics	Total population[a] (n = 30)	AF (11)	No AF (19)
Median age at procedure, y	50.1 (11.7-80.0)	49.6 (35.5-80.0)	51.0 (11.7-71.7)
Male, sex	17 (57)	7	10
CHD	2 (7)	…	2
CAD	2 (7)	2	…
TIA/stroke	2 (7)	1	1
Diagnosis of induced tachyarrhythmia			
Paroxysmal AF	5 (17)	5	…
AFL	2 (7)	1	1
Paroxysmal AF + AFL	2 (7)	2	…
AT	4 (13)	2	2
AVNRT	10 (33)	…	10
AVRT	2 (7)	1	1
VT	1 (3)	…	1
N. I.	4 (13)	…	4
Antiarrhythmic drug class			
IA	2 (7)	1	1
II	8 (27)	6	2
III	8 (27)	2	6
Including amiodarone	5[b] (17)	…	5
IV	4 (13)	2	2

Note: Categorical data are presented as n (%). Characteristics of the study population. The number and percentages are given for the entire study population. The numbers are also given for both patient groups separately (patients without and patients with a history of AF) to visualize similarities and differences. See text for further explanation.
Abbreviations: AF, atrial fibrillation; AFL, atrial flutter; AT, atrial tachycardia; AVNRT, atrioventricular nodal reentrant tachycardia; AVRT, atrioventricular re-entry tachycardia; CAD, coronary artery disease; CHD, coronary heart disease; LVEF, left ventricular ejection fraction; N. I., not inducible; TIA, transient ischemic attack; VT, ventricular tachycardia.
[a]Only patients of which U-AEGMs are included.
[b]All five patients have a history of AF.

by the Wilcoxon signed-rank test, while variability between and within groups was analyzed using analysis of variance. Categorical data were expressed as numbers (%) and analyzed using Pearson χ^2 test when appropriate. $P < .050$ was considered as statistically significant.

3 | RESULTS

3.1 | Study population

A total of 30 patients (18 male; 50 [12-80] years) were included. Patient characteristics are summarized in Table 2. Before the procedure, 11 patients (37%) had documented AF episodes. The majority had a normal left ventricular ejection fraction (LVEF); in four patients, the LVEF was impaired. During the electrophysiological study, diagnosis of the induced tachyarrhythmia was AF (n = 5), atrial flutter (AFL; n = 2), AFL + AF (n = 2), atrial tachycardia (AT; n = 4), atrioventricular nodal reentry tachycardia (AVNRT; n = 10), atrioventricular re-entry tachycardia (AVRT; n = 2), or ventricular tachycardia (n = 1). In four patients, arrhythmias could not be induced. All patients in whom AF was induced, had documented AF episodes before the procedure. None of the patients in whom AVNRT was induced had a history of AF episodes. AFL, AT, and AVRT was equally induced in both groups.

3.2 | Database of U-AEGMs

Table 1 shows the applicability of each of the different APES protocols separately. Seventy-nine percent (n = 356) of the APES attempts (n = 450) was successfully executed and suitable for analysis. The remaining protocols (n = 94; 21%) were excluded due to SR-CL shorter than the CL of the APES protocol (n = 7), repeated occurrence of AR (n = 45; including six times in combination with FFRW), FFRW fusion (n = 10), or accidental induction of AF (n = 4; two times combined with FFRW fusion).

AR varied from 200 to 390 ms (Table 3). AR was significantly longer in the AF group compared to the control group (298 ± 48 vs 255 ± 33 ms; $P \leq .020$). There was no difference in AR between the AF patients with and without amiodarone therapy (278 ± 48 vs 311 ± 40 ms; $P \leq .126$).

The excluded APES protocols contained 2850 U-AEGMs. In addition, 460 individual U-AEGMs (3.4%) were excluded from analysis due to poor signal quality. The final U-AEGM database consisted of 10 504 U-AEGMs (SR: 3872 and APES: 6632). Typical examples of excluded U-AEGMs are shown in Figure 2B.

3.3 | Temporal stability of U-AEGMs

Figure 3 shows the boxplots of SR U-AEGM widths and amplitudes recorded before each of the different APES protocol, depicted per electrode for both the control and the AF group separately. As demonstrated in Table S1, for all recording sites, there were no significant SR U-AEGM differences in width (control group $P \geq .396$; AF group $P \geq .818$) and amplitude (control group $P \geq .969$; AF group $P \geq .561$), indicating stable catheter positions.

3.4 | Impact of fixed-rate stimulation and extra stimuli on U-AEGM morphology

The impact of each of the different APES protocols on Δ width and Δ amplitude of U-AEGMs is shown in Figure 4. Changes in both width and amplitude were most pronounced in the AF group. As demonstrated in Table S2, fixed-rate stimulation decreased the U-AEGM width significantly for all protocols ($P \leq .022$, control vs AF groups; $P = .000$). In contrast, during the shortening of the coupling interval of the extra stimuli, the width increased, but only significantly in protocol 8 ($P \leq .018$, control vs AF groups; $P = .000$).

The amplitude decreased both for fixed-rate stimulation and extra stimuli, and decreased further during shorter coupling intervals (significant: protocols 8 and 13; $P \leq .043$, control vs AF groups; $P \leq .007$).

Figure 5 shows the influence of APES on fractionation (black bars: change from nonfractionated to fractionated U-AEGM, white bars: change from fractionated to nonfractionated U-AEGM) for each protocol separately, applied to the control (upper panel) and AF groups (lower panel). In contrast to the control group, the percentage of fractionation increases with shorter APES (coupling) intervals in the AF group, for fixed-rate stimuli as well as for extra stimuli. Table S2 demonstrates that there is a significant difference in Δ fractionation between both groups for APES protocols 2 and 5

TABLE 3 Shortest effective stimulation intervals[a]

Successive Patient no.	History of AF	Fixed-rate burst S1 with extra stimulus S2 at 8S1 600, ms	8S1 500, ms	8S1 400, ms	Decremental burst, ms
1	X	250	250	250	250
2		250	250	250	250
3		350	350	250	250
4	X	350	NA	350	***310***
5		250	250	250	200
6	X	300	300	300	***220***
7		300	300	300	250
8	X	350	300	NA	NA
9	X	350	350	350	300
10		250	250	250	250
11	X	300	350	300	***390***
12	X	300	300	300	250
13		250	250	300	200
14		NA	250	250	250
15	X	250	250	250	200
16		250	250	250	250
17	X	350	350	350	300
18		250	250	250	250
19		250	250	250	200
20		300	300	300	250
21	X	300	300	250	NA
22		250	250	250	250
23		250	250	300	200
24	X	250	250	250	200
25		250	250	250	200
26		250	250	250	200
27		300	300	NA	200
28		300	350	NA	200
29		NA	250	250	200
30		NA	300	250	200

Note: The shortest effective stimulated intervals observed during the application of the APES protocols are displayed. The shortest interval resulting in atrial capture is given in relation with the details of the specific APES protocol.

Abbreviations: 8S1, train of 8 fixed rate stimuli at given cycle length; NA, not available; S2, extra stimulus.

[a]Stimulation protocols were designed with 50 ms decreasing steps. Some decremental burst protocols were executed with −10 ms steps (*values bold italic*).

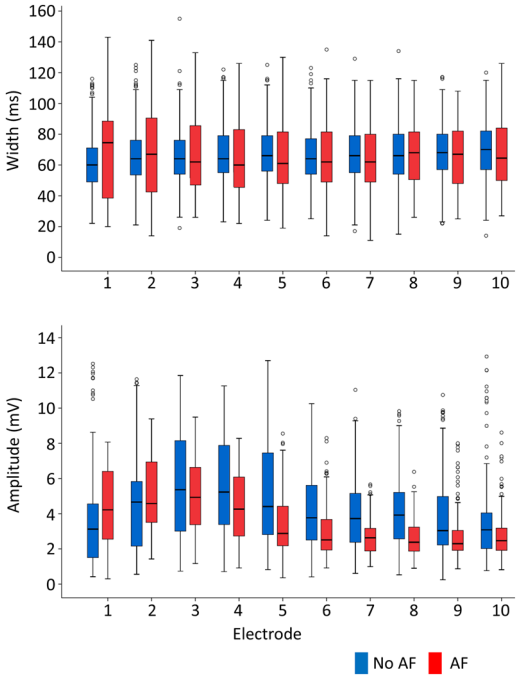

FIGURE 3 Stability of SR U-AEGM widths and amplitudes. Variation in U-AEGM widths (upper panel) and amplitude (lower panel) per each individual electrode no. 1 to 10 are displayed for patients without and with a history of AF separately. AF, atrial fibrillation; SR, sinus rhythm; U-AEGM, unipolar atrial electrogram

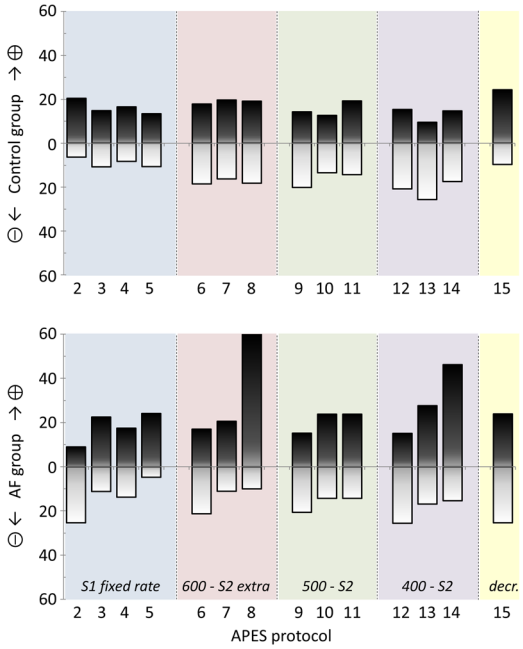

FIGURE 5 Impact of APES protocols on U-AEGM fractionation. The impact of each different APES protocol on U-AEGM fractionation of both the control group (upper panel) and the AF group (lower panel). Black bars represent the change due to APES from no fractionation to fractionation (+), white bars represent a change from fractionation to no fractionation (−). AF, atrial fibrillation; APES, atrial programmed electrical stimulation; U-AEGM, unipolar atrial electrogram

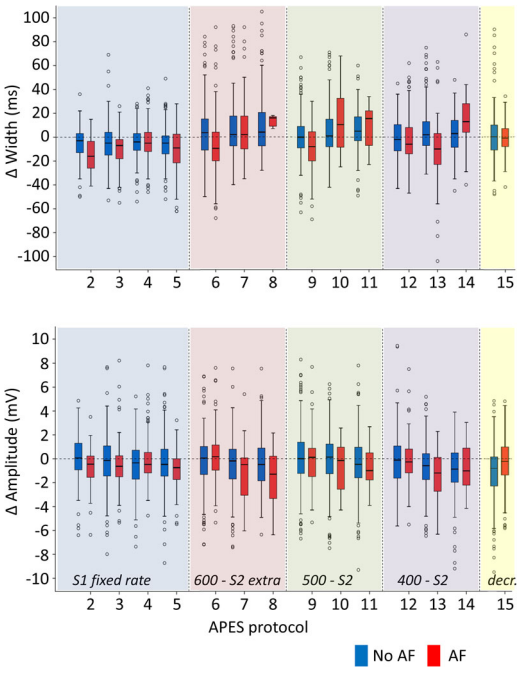

FIGURE 4 Impact of APES protocols on U-AEGM width and amplitude. Δ U-AEGM widths (upper panel) and Δ U-AEGM amplitudes (lower panel) for each separate protocol in the control and AF group. AF, atrial fibrillation; APES, atrial programmed electrical stimulation; U-AEGM, unipolar atrial electrogram

(fixed-rate stimulation, control vs AF groups; $P \leq .045$) and protocols 8, 13, and 14 (extra stimuli, control vs AF groups; $P \leq .014$).

3.5 | Impact of decremental stimulation on U-AEGM morphology

Compared to the SR beat preceding the decremental stimuli, the last captured APES beat resulted in a decreased amplitude and an increased fractionation. These changes differed significantly between the control and the AF group (amplitude −0.81 [−9.50 to 4.85] vs −0.25 mV [−5.83 to 4.82]; $P = .000$ and fractionation 34.1% vs 49.3%; $P = .005$, respectively). Changes in U-AEGM width (control group vs AF group, 0 [−48 to 90] vs −1 ms [−42 to 34]; $P = .571$) were not significant.

3.6 | Optimal APES protocol

The impact of each APES protocol on changes in width, amplitude, and fractionation is summarized in Table 4. On the basis of significances for changes in width, amplitude, and fractionation within and between the control and the AF groups, the most optimal APES protocol unraveling local conduction abnormalities, was protocol 14, which consisted of fixed-rate stimulation with extra stimuli (8S1-S2 = 400-250 ms). Although protocol 7 also showed

TABLE 4 Significances in U-AEGM morphology changes; identification of the most optimal stimulation protocol

	Protocol (ms)	Δ	Δ Width			Δ Amplitude			Δ Fractionation	Significant changes	
			All	AF⊖	AF⊕	All	AF⊖	AF⊕	All	All	AF ⊖ vs AF⊕
1	SR	-									
2	S1 BCL-50	S1-SR	**0.000**	**0.000**	**0.000**	**0.015**	0.439	**0.002**	**0.000**	┼	–
3	S1 500	S1-SR	**0.000**	**0.000**	**0.000**	**0.005**	0.194	**0.001**	0.312	–	–
4	S1 400	S1-SR	**0.000**	**0.000**	**0.022**	**0.001**	**0.005**	0.086	0.379	–	–
5	S1 300	S1-SR	**0.000**	**0.000**	**0.000**	**0.000**	**0.004**	**0.000**	**0.045**	┼	–
6	S1 600-S2 350	S2-SR	0.593	**0.034**	**0.001**	0.909	0.703	0.713	0.857	0	–
7	S1 600-S2 300	S2-SR	**0.006**	**0.013**	0.202	**0.000**	0.061	**0.000**	0.620	–	┼
8	S1 600-S2 250	S2-SR	**0.000**	**0.003**	**0.018**	**0.007**	**0.043**	**0.041**	**0.014**	┼	–
9	S1 500-S2 350	S2-SR	**0.034**	0.766	**0.000**	0.839	0.888	0.693	0.967	–	–
10	S1 500-S2 300	S2-SR	0.066	0.151	0.200	0.471	0.978	0.086	0.184	0	0
11	S1 500-S2 250	S2-SR	**0.000**	**0.000**	0.073	**0.018**	0.059	0.199	0.890	–	–
12	S1 400-S2 350	S2-SR	0.192	0.832	0.118	0.112	0.224	0.318	0.694	0	0
13	S1 400-S2 300	S2-SR	0.983	**0.010**	**0.001**	**0.000**	**0.000**	**0.000**	**0.002**	–	–
14	S1 400-S2 250	S2-SR	**0.003**	0.129	**0.002**	**0.000**	**0.000**	0.104	**0.002**	┼	┼
15	Decremental 600-50	S_x-S_{x-1}	0.571	0.586	0.942	**0.000**	**0.000**	0.224	**0.005**	–	–

Note: Values are bold when $P \leq .50$. ┼, significant in all; –, significant in one or two; 0, significant in none of the parameters. Due to defined binomin al nature of fractionation, values for AF⊖ and AF⊕ are not available. Significance of the impact of each APES protocol on the U-AEGM morphology (including width, amplitude, and fractionation) for the entire study population and for patients without and patients with a history of AF separately. The right column displays in which protocols overall morphological changes, and changes between patients without and with a history of AF, were significant. Abbreviations: AF⊖, patients without a history of atrial fibrillation; AF⊕, patients with a history of AF; BCL, basic cycle length; S1, train of fixed-rate stimulation at given cycle length; S2, single extra stimulus at given cycle length; SR, sinus rhythm; U-AEGM, unipolar atrial electrogram.

significant differences between the control group and the AF group, changes in fractionation, however, were not significant.

4 | DISCUSSION

In this study, we compared the impact of APES techniques on U-AEGM morphology between patients without (control group) and with a history of AF. From our data, it appeared that the most optimal stimulation protocol for unraveling local conduction abnormalities reflected by significant U-AEGM changes in morphology (width, amplitude, and fractionation) consists of fixed-rate stimulation at a drive train of 400 ms followed by extra stimuli with a coupling interval of 250 ms. This study is the first step towards examining the value of APES for the detection of AF-related conduction disorders.

4.1 | Changes in U-AEGM morphology related to stimulation sequence—interval and AF

U-AEGM morphology during SR did not change over time, demonstrating stable catheter positions. This enabled us to compare U-AEGM morphology changes recorded during APES with the preceding SR U-AEGMs.

Electrogram (EGM) width is inversely related to the conduction velocity (CV). Prior studies demonstrated that slowing of conduction in the left atrial (LA) precedes the initiation of AF, and this, in turn, is related to increased AF vulnerability and persistence.[18,19] In various animal models, AR and CV decreased, while AF inducibility and duration increased, but these results were measured after days of long-lasting fixed high-rate atrial stimulation.[20,21] During fixed-rate stimulation with extra stimuli, we found an increasing U-AEGM width when the coupling interval was shortened. However, we observed an acute decrease in U-AEGM width during fixed-rate APES. The measurements during fixed-rate APES in this study were taken shortly (within seconds) after the start of stimulation (S1) (or directly from the extra stimulus (S2), with only eight preceding S1 beats), and SR recovered between the different APES protocols. Although adaptation of the action potential duration (APD) to an elevated (stimulation) rate starts immediately after the CL changes, it reaches a new steady state only after at least 30 seconds.[22] The same will apply to the ECG width. Thus, in this study, measurements were taken during nonsteady state conditions. Because the AR is correlated to the APD,[23] this, in turn, made it unlikely that the results of this study could have been influenced by decreased AR rate adaptation due to prolonged elevated stimulation rates.

In addition, in contrast to the studies mentioned above, none of the patients in this study had a history of long-standing persistent AF, when structural remodeling (with even advanced slowing of conduction due to increasing anisotropy) has become more pronounced.

We observed that the U-AEGM amplitudes in the AF group during SR and during APES are lower compared to the control group, and amplitudes decrease with decreasing APES intervals, also especially in patients with a history of AF.

Lower atrial EGM amplitudes have frequently been observed in LA voltage maps in patients with AF undergoing endovascular pulmonary vein isolation procedures.[24,25] It is generally assumed that

decreased EGM amplitudes correlate with advanced fibrosis of atrial tissue. While most authors used bipolar EGM recording techniques, this study confirms that amplitudes of unipolar atrial potentials are also decreased in patients with AF.

In this study, fractionation did not increase in the control group, while it increased with decreasing APES intervals in the AF group. These changes occurred during fixed-rate stimulation, stimulation with extra stimuli, as well as during decremental stimulation. These findings are comparable with earlier observations of slowing of conduction and increasing signal complexity (fractionation) in patients with AF.[26,27] In line with previous studies, we also found an association between decreased U-AEGM amplitudes and increased fractionation.[19]

The results of this study add more insight to how APES affects the unipolar morphology. This is important, because bipolar recording has its limitations for morphological characterization of tissue conduction properties.[28,29] To the best of our knowledge, no studies on the influence of electrical stimulation on the unipolar EGM morphology have been published. Our results showed similar findings for unipolar EGM amplitude and fractionation. However, we found that a relation between width and fractionation is less pronounced than expected from studies based on the bipolar recording. We suppose that the interaction of both discrete recording pole signals during bipolar EGM recording is accountable for differences found between unipolar and bipolar EGM.

In addition, while most studies focussed on the LA,[15,18,19,26] the results of this study show that conduction abnormalities are not limited to the LA alone, but can also be detected in the right atrial (RA).[8,27]

We found differences in U-AEGM morphology during APES between patients without and with a history of AF. Although this could be expected, it was not the aim of this study. No further research into the patient-specific differences between these groups was conducted. In this study, the protocol of 8S1-S2 at 400-250 ms demonstrated the most significant morphological changes between both groups. This shows that during acute measurements, at least a relatively fast APES protocol with an extra stimulus close to AR (8S1-S2) is needed to unmask these differences. We assume that both reduced rate adaptation ability and AR in patients with (a history of) AF play a major role, and that a marked difference between S1 and S2 is needed, especially during acute measurements. However, the effectiveness of APES decreases when S2 approaches AR, so this can be a limitation of the usefulness of APES for the detection of AF-related conduction abnormalities.

4.2 | Study limitations

Occasionally, not all the APES protocols could be applied to all patients due to unintended induction of AF. We examined only one stimulation and one recording catheter position. Multisite high-resolution recording and stimulation is needed to address regional and directional influences of APES on U-AEGM morphology.[29] The degree of contact of the recording electrodes with the atrial wall during APES remains uncertain which could have influenced U-AEGM morphology, in particular the amplitude. Nevertheless, our findings on changes in U-AEGM width, amplitude, and fractionation during APES were consistent with each other.

5 | CONCLUSION

This electrophysiology study in the RA shows that APES results in significant changes in U-AEGM morphology including width, amplitude, and fractionation, which were more pronounced in patients with a history of AF. Fixed-rate stimulation with an extra stimulus at a relatively fast rate (8S1-S2 at 400-250 ms) was the most optimal APES protocol to reveal morphological changes in the U-AEGM. This study supports the concept that dedicated APES is useful to unmask conduction abnormalities which may be related to AF; however, further research is necessary to clarify its value for the individual patient.

ACKNOWLEDGMENT

The authors would like to thank the staff of the Erasmus MC EP Department for their assistance during the execution of the stimulation protocols and collection of the EGM data. Dr Natasja de Groot is supported by funding grants from the Erasmus Medical Center fellowship, Dutch Heart Foundation (2012T0046), CVON-AFFIP (914728), and NWO-Vidi (91717339). This study (IIS-331 Phase 1) was conducted with financial support from the Investigator-Initiated Study Program of Biosense Webster Inc.

ORCID

Natasja de Groot http://orcid.org/0000-0002-0259-6691

REFERENCES

1. Mouws EMJP, van der Does LJME, Kik C, et al. Impact of the arrhythmogenic potential of long lines of conduction slowing at the pulmonary vein area. *Heart Rhythm*. 2019;16:511-519.
2. Konings KT, Kirchhof CJ, Smeets JR, Wellens HJ, Penn OC, Allessie MA. High-density mapping of electrically induced atrial fibrillation in humans. *Circulation*. 1994;89:1665-1680.
3. Allessie MA, de Groot NMS, Houben RPM, et al. Electropathological substrate of long-standing persistent atrial fibrillation in patients with structural heart disease: longitudinal dissociation. *Circ Arrhythm Electrophysiol*. 2010;3:606-615.
4. de Groot NMS, Houben RPM, Smeets JL, et al. Electropathological substrate of longstanding persistent atrial fibrillation in patients with structural heart disease: epicardial breakthrough. *Circulation*. 2010; 122:1674-1682.
5. Yaksh A, van der Does LJ, Kik C, et al. A novel intra-operative, high-resolution atrial mapping approach. *J Interv Card Electrophysiol*. 2015;44:221-225.
6. Konings KT, Smeets JL, Penn OC, Wellens HJ, Allessie MA. Configuration of unipolar atrial electrograms during electrically induced atrial fibrillation in humans. *Circulation*. 1997;95:1231-1241.
7. Teuwen CP, Yaksh A, Lanters EAH, et al. Relevance of conduction disorders in bachmann's bundle during sinus rhythm in humans. *Circ Arrhythm Electrophysiol*. 2016;9:e003972.
8. Lanters EAH, Yaksh A, Teuwen CP, et al. Spatial distribution of conduction disorders during sinus rhythm. *Int J Cardiol*. 2017;15:220-225.

9. Saumarez RC, Camm AJ, Panagos A, et al. Ventricular fibrillation in hypertrophic cardiomyopathy is associated with increased fractionation of paced right ventricular electrograms. *Circulation*. 1992;86:467-474.
10. Saumarez RC, Chojnowska L, Derksen R, et al. Sudden death in noncoronary heart disease is associated with delayed paced ventricular activation. *Circulation*. 2003;107:2595-2600.
11. Saumarez RC, Grace AA. Paced ventricular electrogram fractionation and sudden death in hypertrophic cardiomyopathy and other noncoronary heart diseases. *Cardiovasc Res*. 2000;47:11-22.
12. Saumarez RC, Pytkowski M, Sterlinski M, et al. Paced ventricular electrogram fractionation predicts sudden cardiac death in hypertrophic cardiomyopathy. *Eur Heart J*. 2008;29:1653-1661.
13. Saumarez RC, Pytkowski M, Sterlinski M, et al. Delayed paced ventricular activation in the long QT syndrome is associated with ventricular fibrillation. *Heart Rhythm*. 2006;3:771-778.
14. Saumarez RC, Slade AK, Grace AA, Sadoul N, Camm AJ, McKenna WJ. The significance of paced electrogram fractionation in hypertrophic cardiomyopathy. A prospective study. *Circulation*. 1995;91:2762-2768.
15. Roberts-Thomson KC, Stevenson IH, Kistler PM, et al. Anatomically determined functional conduction delay in the posterior left atrium. Relationship to structural heart disease. *J Am Coll Cardiol*. 2008;51:856-862.
16. van der Does LJ, de Groot NM. Inhomogeneity and complexity in defining fractionated electrograms. *Heart Rhythm*. 2017;14:616-624.
17. van der Does LJME, Knops P, Teuwen CP, et al. Unipolar atrial electrogram morphology from an epicardial and endocardial perspective. *Heart Rhythm*. 2018;15:879-887.
18. Lalani GG, Schricker A, Gibson M, Rostamian A, Krummen DE, Naraya SM. Atrial Conduction Slows Immediately Before the Onset of Human Atrial Fibrillation. A Bi-Atrial Contact Mapping Study of Transitions to Atrial Fibrillation. *J Am Cardiol*. 2012;59:595-606.
19. Narayan SM, Franz MR, Clopton P, Pruvot EJ, Krummen DE. Repolarization Alternans Reveals Vulnerability to Human Atrial Fibrillation. *Circulation*. 2011;123:2922-2930.
20. Gaspo R, Bosch RF, Talajic M, Nattel S. Functional Mechanisms Underlying Tachycardia-Induced Sustained Atrial Fibrillation in a Chronic Dog Model. *Circulation*. 1997;96:4027-4035.
21. Monigatti-Tenkorang J, Jousset F, Pascale P, et al. Intermittent Atrial Tachycardia Promotes Repolarization Alternans and Conduction Slowing During Rapid Rates, and Increases Susceptibility to Atrial Fibrillation in a Free-Behaving Sheep Model. *J Cardiovasc Electrophysiol*. 2014;25:418-427.
22. Hara M, Shvilkin A, Rosen MR, Danilo P Jr, Boyden PA. Steady-state and nonsteady-state action potentials in fibrillating canine atrium: abnormal rate adaptation and its possible mechanisms. *Steady-state and nonsteady-state action potentials in fibrillating canine atrium: abnormal rate adaptation and its possible mechanisms. Cardiovasc Res*. 1999;42:455-469.
23. Bode F, Kilborn M, Karasik P, Franz MR. The repolarization-excitability relationship in the human right atrium is unaffected by cycle length, recording site and prior arrhythmias. *J Am CC*. 2001;37:920-925.
24. Rolf S, Kircher S, Arya A, et al. Tailored atrial substrate modification based on low-voltage areas in catheter ablation of atrial fibrillation. *Circ Arrhythm Electrophysiol*. 2014;7:825-833.
25. Masuda M, Fujita M, Iida O, et al. Comparison of left atrial voltage between sinus rhythm and atrial fibrillation in association with electrogram waveform. *Pacing Clin Electrophysiol*. 2017;40:559-567.
26. Walters TE, Teh AW, Spence S, Kistler PM, Morton JB, Kalman JM. Relationship between the electrocardiographic atrial fibrillation cycle length and left atrial remodeling: a detailed electroanatomic mapping study. *Heart Rhythm*. 2014;11:670-676.
27. Starreveld R, van der Does LJME, de Groot NMS. Anatomical hotspots of fractionated electrograms in the left and right atrium; do they exist? *Europace*. 2019;21:60-72.
28. de Bakker JM, Wittkampf FH. The pathophysiologic basis of fractionated and complex electrograms and the impact of recording techniques on their detection and interpretation. *Circ Arrhythm Electrophysiol*. 2010;3:204-213.
29. Williams SE, Linton N, O'Neill L, et al. The effect of activation rate on left atrial bipolar voltage in patients with paroxysmal atrial fibrillation. *J Cardiovasc Electrophysiol*. 2017;28:1028-1036.

SUPPORTING INFORMATION

Additional supporting information may be found online in the Supporting Information section.

How to cite this article: Knops P, Schram-Serban C, van der Does L, Croes M, Houben R, de Groot N. Impact of atrial programmed electrical stimulation techniques on unipolar electrogram morphology. *J Cardiovasc Electrophysiol*. 2020;31:943–951. https://doi.org/10.1111/jce.14394